Semana de Engenharia 2010
Guimarães, 11 a 15 de Outubro

FLEXURAL STRENGHENING OF RC CONTINUOUS SLAB STRIPS USING NSM CFRP LAMINATES

Gláucia Dalfré and Joaquim Barros
ISISE - Department of Civil Engineering
E-mail: gmdalfre@civil.uminho.pt

KEYWORDS
Continuous RC slabs, Flexural strengthening, CFRP, NSM, Moment redistribution.

ABSTRACT

An ongoing investigation on the use of the Near Surface Mounted (NSM) CFRP laminates for the flexural strengthening of continuous Reinforced Concrete (RC) slabs is being carried out in order to verify the possibility of increasing the negative resisting bending moment in 25% and 50% and maintaining moment redistribution levels of 15%, 30% and 45%.
To better understand the behaviour of these structures, a comprehensive experimental program is being conducted with the aim of evaluating the possibilities of the NSM technique for statically indeterminate RC slab strips in terms of flexural strengthening effectiveness, moment redistribution and ductility performance.

INTRODUCTION

In general, when a structural Reinforced Concrete (RC) element is strengthened with fiber reinforced polymer (FRP) systems, its failure mode tends to be more brittle than its unstrengthened homologous element, due to the intrinsic bond conditions between these systems and the concrete substrate, as well as the linear-elastic brittle tensile behavior of FRPs. In case of continuous RC slabs and beams (statically indeterminate structures), the use of FRP systems to increase their flexural resistance can even compromise the moment redistribution capacity of these types of elements.Externally Bonded Reinforcement, EBR (ACI 440 2007, FIB 2001), and the Near Surface Mounted, NSM (Barros and Kotynia 2008; Barros et al. 2007) are the most used techniques for the strengthening of RC elements. However, when compared to EBR, the NSM technique is especially appropriate to increase the negative bending moments (in the intermediate supports) of continuous RC slabs since its strengthening process is simpler and faster to apply than other FRP-based techniques (Barros and Kotynia 2008). The efficiency of the NSM technique for the flexural (Barros and Fortes 2005; De Lorenzis et al. 2000; Liu et al. 2006) and shear (Barros and Dias 2006, Dias and Barros 2008, Dias and Barros 2010; Anwarul Islam 2009) strengthening of RC members has already been assessed. However, most of the tests were carried out with simply supported NSM strengthened members.

Although many in situ RC elements are of continuous construction, there is a lack of experimental and theoretical studies in the behavior of statically indeterminate RC members strengthened with FRP materials. Related to the analysis of the behavior of continuous elements, the majority of research studies reports the use of EBR technique. Limited information is available in literature dealing with the behavior of continuous structures strengthened according to the NSM technique (Liu 2005; Liu et al. 2006; Bonaldo 2008).
In the present paper the potentialities of the NSM technique are explored for the increase of the load carrying capacity of two spans continuous RC slabs. The NSM strengthening configurations applied in the slab strip were designed to increase in 25% the load carrying capacity of its corresponding unstrengthened reference RC slab, maintaining a moment redistribution level of about 30%.

EXPERIMENTAL PROGRAM

Specimen and Test Configuration

The experimental program is composed by the two RC slab strips with the geometry, support and load conditions, reinforcement and strengthening arrangements represented in Figure 1.

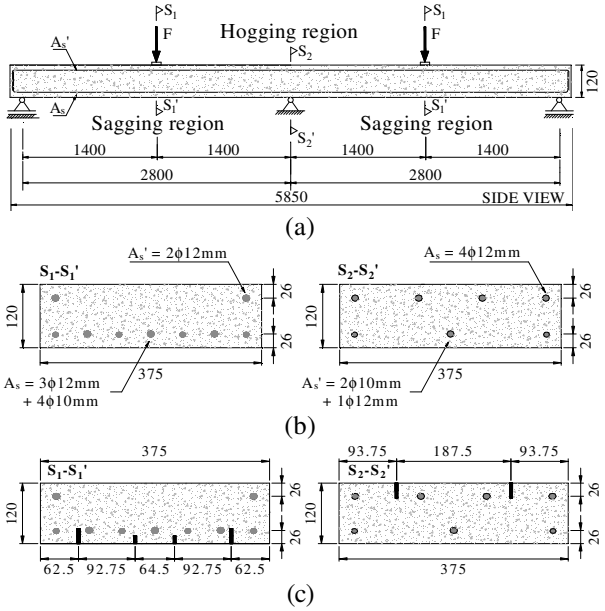

Figure 1: Slab strips: (a) test configuration, (b and c) cross-sectional dimensions at sagging (S1-S1') and hogging regions (S2-S2'). All dimensions are in mm.

The steel reinforcement arrangements in the reference slab (with the designation of SL30) were designed for a load of 46.2 kN, which is the load that introduces a deflection of L/480 (L=2800 mm is the span length of the slab) recommended by the ACI 318 (2004), and assuming a moment redistribution of 30%. Furthermore, in the evaluation of these reinforcement arrangements a strain limit of 3.5‰ for the concrete crushing was assumed.

According to the CEB-FIB Model Code (1993), the coefficient of moment redistribution, $\delta = M_{red}/M_{elas}$, is defined as the relationship between the moment in the critical section after redistribution (M_{red}) and the elastic moment (M_{elas}) in the same section calculated according to the theory of elasticity, while $\eta = (1-\delta)\cdot 100$ is the moment redistribution percentage. The NSM flexural strengthened slab has the same steel reinforcement arrangement adopted in the reference slab, and a number of CFRP laminates applied in the hogging (intermediate support) and sagging regions (loaded zones) designed in order to increase the load carrying capacity of the reference slab (REF) in 25%.

The design of cross sections subject to flexure was based on stress and strain compatibility, where the maximum strain at extreme concrete compression fiber was assumed equal to 0.0035.

In order to increase the load carrying capacity in 25% the strengthening arrangement represented in Figure 1(c) was adopted. In the hogging region, two 1.4×20 mm^2 cross section area CFRP laminates were applied, while in both sagging regions two 1.4×20 mm^2 and two 1.4×10 mm^2 CFRP laminates were installed. This slab has the designation of SL30s25.

The test with the strengthened slab strip had two phases. In the first phase the slab was loaded up to attain in the loaded sections a deflection corresponding to 50% of the deflection measured in the reference slab when steel reinforcement in the hogging region (H) has attained its yield strain. When attained this deflection level (5.8 mm), a temporary reaction system was applied in order to maintain this deformability during the period necessary to strengthen the slab. To control the maintenance of this deflection, dial gauges were used in order to adjust the temporary reaction system when necessary. Therefore, the strengthening process was applied maintaining the slab with a damage level that can be representative of real slabs requiring structural rehabilitation. After the curing time of the adhesives used to bond the NSM CFRP strips (which in general took about two weeks), the temporary reaction system was removed, while the load was transferred to the slab. This stress transfer process was governed by the criteria of maintaining the deflection level that corresponds to the initiation of the second phase of the test (5.8 mm). This second phase ended when the strengthened slab strip has ruptured.

Measuring devices

The slab strips were carefully monitored in order to provide relevant information, not only for the efficacy of the technique but also for the appraisal of the analytical formulation and numerical models to be applied for the prediction of the behaviour of the strengthened RC elements. Figure 2 depicts the positioning of the sensors for data acquisition in the tests. To measure the vertical deflection of a slab strip, six linear voltage differential transducers (LVDT 82803, LVDT 60541, LVDT 82804, LVDT 19906, LVDT 18897 and LVDT 3468) were supported in a suspension bar (Figure 2a). The LVDTs 60541 and 18897, placed at the slab loaded sections, were also used to control the test at a displacement rate of 10 µm/s up to the deflection of 50 mm. After this deflection, the internal LVDTs of the actuators were used to control the test at a displacement rate of 20 µm/s up to the failure of the slab strip.

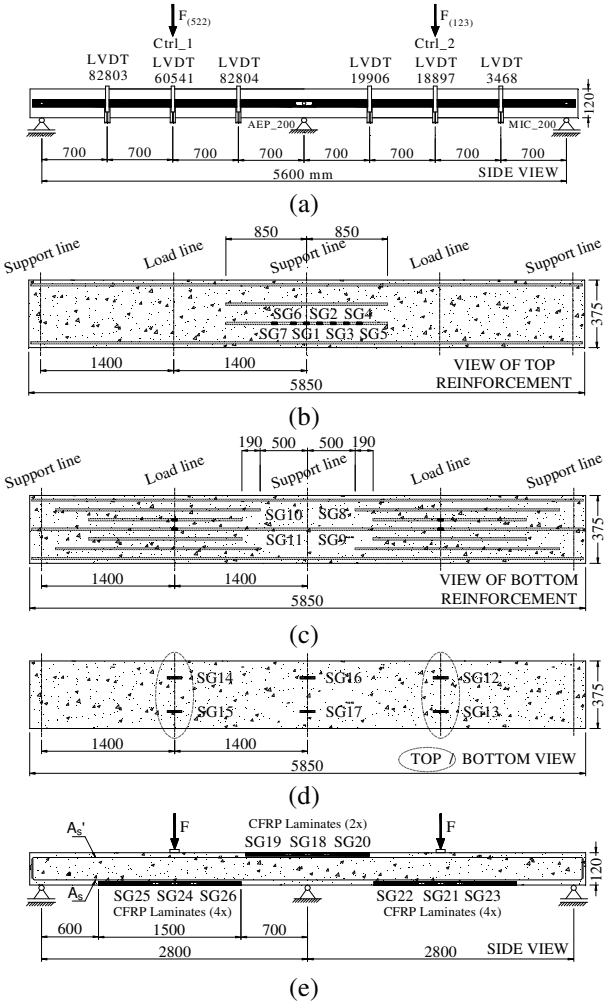

Figure 2: Arrangement of displacement transducers and strain gauges: (a) displacement transducers; layout of strain gauges at steel bars at hogging (b) and sagging (c) region; (d) strain gauges at concrete slab surfaces, (e) layout of strain gauges at CFRP laminates for SL30s25 (all dimensions are in mm).

The load ($F_{(522)}$) applied at the left span (Figure 2a) was measured using a load cell of ±200 kN and accuracy of ±0.03% (designated Ctrl_1), placed between the loading steel frame and the actuator of 150 kN load capacity and 200 mm range. In the right span, the load ($F_{(123)}$) was applied with an actuator of 100 kN and 200 mm range, and the corresponding force was measured using a load cell of ±250 kN and accuracy of ±0.05% (designated Ctrl_2). To monitor the reaction forces, load cells were installed under two supports. One load cell (AEP_200) was positioned at the central support (nonadjustable support), placed between the reaction steel frame (HEB 300 profile) and the slab's support device (Fig. 2a). The other load cell (MIC_200) was positioned in-between the reaction steel frame and the apparatus of the adjustable right support of the slab. These cells have a load capacity of 200 kN and accuracy of ±0.05%.

To monitor the strain variation in the steel bars, concrete and CFRP laminates, the arrangements of strain gauges (SGs) represented in Figure 2(b-e) were adopted. Eleven SGs were installed in steel bars, seven of them in steel bars at top surface in the hogging region (SG1 to SG7) and the other four in steel bars at bottom surface in the sagging regions (SG8 to SG11, Figure 2b-c). Six SGs were applied at the external concrete surface in the compression regions (SG12 to SG17, Figure 2d). Finally, three SGs (SG18 to SG20) were bonded along one CFRP laminate in the hogging region and three SGs (SG21 to SG23 and SG24 to SG26) were installed along one CFRP laminate in both sagging regions (Figure 2e).

Material Properties

Tables 1 to 3 include values obtained from experimental tests for the characterization of the main properties of the materials used in the present work. The compressive strength and the static modulus of elasticity in compression were determined according to NP-E397 (1993).

To characterize the steel bars, uniaxial tensile tests were conducted according to the standard procedures of ASTM A370 (2002). Unidirectional pultruded CFRP laminates, supplied by "S&P Clever Reinforcement Ibérica Company" were used in this study and their tensile behaviour was assessed by performing uniaxial tensile tests carried out according to ISO 527-1 (1993) and ISO 527-5 (1993) recommendations. Both CFRP laminates have a width of 1.4 mm.

For the characterization of the tensile behaviour of the epoxy adhesive, uniaxial tensile tests were performed complying with the procedures outlined in ISO 527-2 (1993). For the adhesive, an elasticity modulus and a tensile strength of 18.60 GPa (11.46%), and 21.12 MPa (6.06%) were obtained, respectively, where the values between round brackets correspond to the coefficient of variation.

Strengthening system

The first step of the NSM strengthening process consisted in opening the slits for the installation of the CFRP laminates, by using a conventional diamond saw cut machine. The slits had a width that varied between 4.5 mm and 4.6 mm and a depth of 15 mm or 27 mm, depending on the depth of the cross section of the used CFRP laminate, 10 mm or 20 mm, respectively. In order to eliminate the dust resultant from the sawing process, the slits were cleaned using compressed air before bonding the laminates to the concrete into the slits. The CFRP laminates were cleaned with acetone to remove any possible dirt. Finally, the slits were filled with the epoxy adhesive using a spatula, and the CFRP laminates were introduced into the slits.

Table 1: Characteristics of plain concrete.

Slab strip	Property	
	f_{cm} (MPa)	E_c (GPa)
SL30	30.10 (1.08)	31.52 (0.86)
SL30s25	32.59 (1.15)	30.62 (2.42)
(value) = Standard deviation		

Table 2: Summary of the properties of steel reinforcement.

Steel bar diameter (ϕs)	Modulus of Elasticity (GPa)	Yield stress (0.2%)[a] (MPa)	Strain at yield stress[b]	Tensile strength (MPa)
10 mm	178.24 (2.48%)	446.95 (3.25%)	0.0027 (0.45%)	575.95 (0.34%)
12 mm	198.36 (2.77%)	442.47 (2.87%)	0.0024 (0.19%)	539.88 (1.84%)
[a]Yield stress determined by the "Offset Method" ASTM A370 (2002), [b]Strain at yield point, for the 0.2% offset stress (value) Coefficient of Variation (COV) = (Standard deviation/Average) x 100				

Table 3: Summary of the properties of CFRP laminates.

CFRP laminate height	Ultimate tensile stress (MPa)	Ultimate tensile strain (‰)	Modulus of Elasticity (GPa)
10 mm	2867.63 (3.07%)	17.67 (3.04%)	159.30 (3.15%)
20 mm	2782.86 (2.73%)	17.76 (3.13%)	156.69 (0.73%)
(value) Coefficient of Variation (COV) = (Standard deviation/Average) x 100			

RESULTS OF THE EXPERIMENTAL PROGRAM

The applied loads ($F_{(522)}$ or $F_{(123)}$) versus deflection curves of the tested slab strips are presented in Figures 3 and 4. Additionally, Table 4 presents the main results obtained experimentally.

In this Table, $\overline{F}_{max}$ is the average load ($\overline{F}_{max} = \left(F_{(522)} + F_{(123)}\right)/2$), $R_{L,\overline{F}_{max}}$ is the load registered at the load cell (MIC_200) and $\Delta\overline{F}_{max}/\overline{F}_{max}^{REF}$ is the increase in terms of load carrying capacity provided by the strengthening technique at $\overline{F}_{max}$.

It can be noted that the adopted NSM strengthening configuration conducted to a significant increase of the load carrying during the second phase of the test loading process. Four phases occurred during each test in the following sequence: a) the uncracked elastic response; b) crack propagation in the hogging and sagging regions with steel bars in elastic stage; c) yielding of the steel reinforcement at the hogging region and crack propagation in the sagging regions with steel bars in elastic stage; d) yielding of the steel reinforcement at the hogging and sagging regions.

As expected, the unstregthened control slab strip behaved in a perfectly plastic manner in the post-yielding phase (after the formation of plastic hinges at hogging and sagging regions), whereas the strengthened slab strips exhibited continuous hardening up to failure.

The failure mechanism of the reference slab was governed by flexure failure mode, i.e. by yielding of internal reinforcements, with extensive cracking in the tension flange, followed by concrete crushing in compression parts.

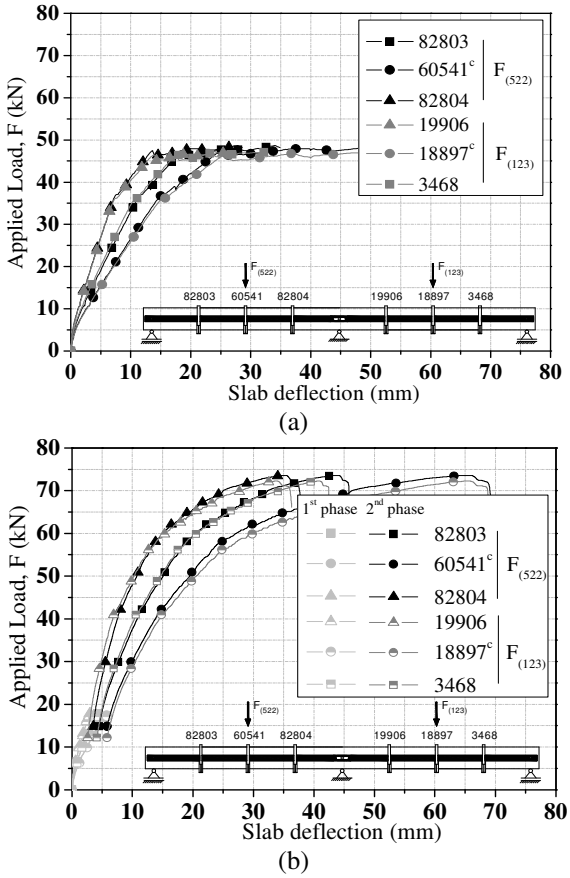

Figure 3: Load-deflection curves: (a) SL30 and (b) SL30s25.

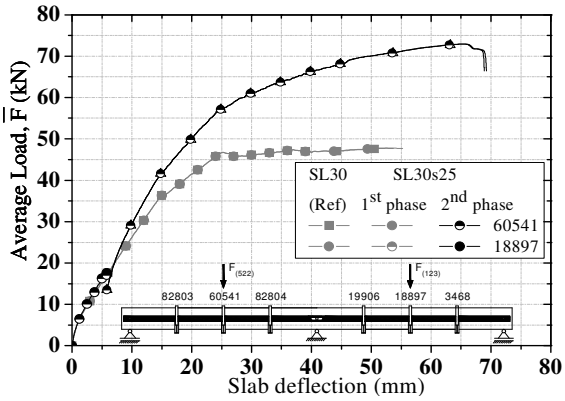

Figure 4: Load-midspan deflection.

Table 4: Main results of the experimental program.

Slab strips ID	$\overline{F}_{max}$ kN	$R_{L,\overline{F}_{max}}$ kN	$\frac{\Delta\overline{F}_{max}}{\overline{F}_{max}^{REF}}$ (%)
SL30	47.85	16.43	-----
SL30s25	72.96	26.19	52.47

The SL30s25 failed by the detachment of the top concrete cover that includes the laminates in the hogging region (Figure 5 a2). Upon further loading, several flexural cracks formed over the hogging region of both slabs, as shown in Figure 5. The number of flexural cracks has increased with the load, and herringbone cracks formed in the concrete surrounding the CFRP laminates at hogging region.

From the analysis of the results it can be outlined the following: 1) For a compressive strain of 3.5‰, the increase of the load carrying capacity provided by the strengthening system was of about 29%; 2) The moment redistribution percentage for a compressive strain of 3.5‰ (at the sagging region) and at $\overline{F}_{max}$ was 21% and 27% for the SL30s25, which are lower that the target limit, but still quite high values.

NUMERICAL SIMULATION

For the prediction of the behaviour of RC continuous slabs strengthened with NSM laminate arrangements capable of increasing the load carrying capacity and assuring high level of moment redistribution for this type of structure, a computer program, based on the finite element method (FEM), was used.

Constitutive laws

According to the present model, a concrete slab is considered a plane shell formulated under the Reissner-Mindlin theory (Barros 1995). In order to simulate the progressive damage induced by concrete cracking and concrete compression nonlinear behavior, the thickness a shell element was discretized in 20 layers that were considered in a state of plane stress. More details can be found elsewhere (Barros et al. 2008).

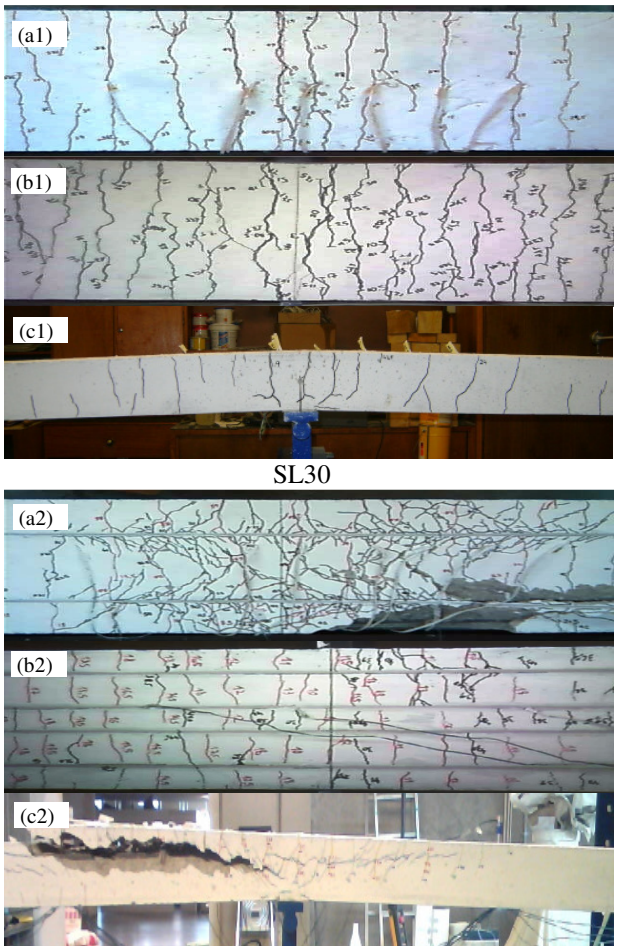

Figure 5: Crack patterns: plant view at hogging (a1-a2) and sagging regions (b1-b2); lateral view (c1-c2) at hogging region.

Steel constitutive law

For modelling the behaviour of the steel bars, the stress-strain relationship represented in Figure 6 was adopted (Sena-Cruz 2004). The curve (under compressive or tensile loading) is defined by the points $PT1=(\varepsilon_{sy},\sigma_{sy})$, $PT2=(\varepsilon_{sh},\sigma_{sh})$ and $PT3=(\varepsilon_{su},\sigma_{su})$, and a parameter p that defines the shape of the last branch of the curve. Unloading and reloading linear branches with slope E_s are assumed in the present approach.

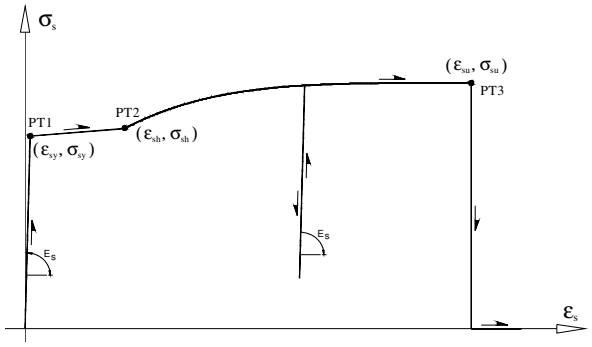

Figure 6: Uniaxial constitutive model for the steel bars.

FRP constitutive law

A linear elastic stress-strain relationship was adopted to simulate the behaviour of NSM CFRP laminates applied in the RC slabs.

Simulation of the tests

Materials properties

Tables 5 and 6 include the values of the parameters adopted for the characterization of the constitutive models for the steel and concrete, respectively. The CFRP laminates were assumed as an isotropic material with an elasticity modulus of 156 GPa and null value for the Poisson's coefficient, since the consideration of their real anisotropic properties have marginal influence in terms of their contribution for the behaviour of NSM strengthened RC slabs.

Table 5: Values of the parameters of the steel constitutive model (see Figure 6).

Steel bar diameter	10 mm	12 mm
PT1 $\begin{pmatrix}\varepsilon_{sy}[-]\\ \sigma_{sy}(MPa)\end{pmatrix}$	2.50×10^{-3} 446.00	2.50×10^{-3} 445.00,
PT2 $\begin{pmatrix}\varepsilon_{sh}[-]\\ \sigma_{sh}(MPa)\end{pmatrix}$	3.07×10^{-2} 446.00	3.05×10^{-2} 445.00
PT3 $\begin{pmatrix}\varepsilon_{su}[-]\\ \sigma_{su}(MPa)\end{pmatrix}$	1.31×10^{-1} 557.50	1.02×10^{-1} 547.35
E_s (GPa)	178.24	198.36

Table 6: Values of the parameters of the concrete constitutive model (Barros et al. 2008)

Poisson´s ratio (ν_c)	0.15
Initial Young´s modulus (E_c)	29.83 GPa
Compressive strength (f_c)	28.40 MPa
Strain at peak compression stress	$\varepsilon_{c,1} = 1.98\times10^{-3}$
Parameter defining the initial yield surface (Sena-Cruz 2004)	$\alpha_0 = 0.4$
Tri-linear tension softening/stiffening diagram	$f_{ct} = 1.50$ MPa $G_f = 0.052$ N/mm $\xi_1 = 0.015$; $\alpha_1 = 0.6$ $\xi_2 = 0.2$; $\alpha_2 = 0.25$
Parameter defining the mode I fracture energy available to the new crack (Barros 1995)	$n = 2$
Shear retention factor	$p_1 = 2$
Crack band-width	Square root of the area of gauss integration point
Threshold angle (Barros 1995)	$\alpha_{th} = 30°$
Maximum number of cracks per integration point	2

Results and discussion

Figures 7 to 12 represent relevant results of the numerical simulations corresponding to the slabs of the SL30 series.
The figures show that the numerical model is able to capture with good accuracy the behaviour of the constituent materials of this structural system during the loading process of the tested slabs.

Moment Redistribution Analysis

The percentages of moment redistribution obtained numerically for the slab strips are shown in Figure 13, where F_{cr} is the cracking load, F_y^H and F_y^S are the loads at the formation of the plastic hinge in the hogging and sagging regions, respectively.
The SL30 slab strip exhibited a moment redistribution rate of about 8.84% at the yielding of steel reinforcement at the central support section. At the yielding of reinforcement at the sagging region, the moment redistribution increased to about 22.7%. For a compressive strain of 3.5‰ at H and S, moment redistribution rates of about 22.74% and 26.88% were obtained, respectively.
Concerning to SL30s25 slab strip, a moment redistribution of 8.49% was obtained when the steel reinforcement has yielded at the hogging region.

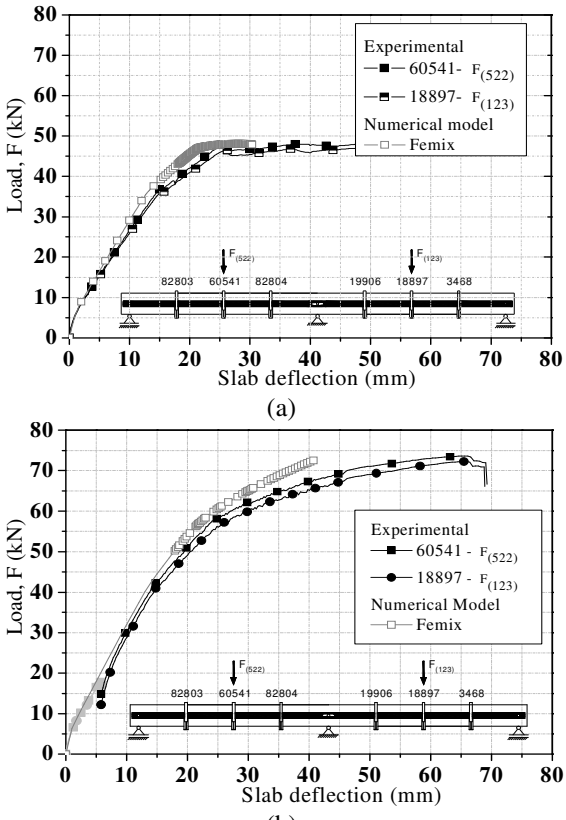

Figure 7: Force-loaded section deflection relationship: (a) SL30 and (b) SL30s25.

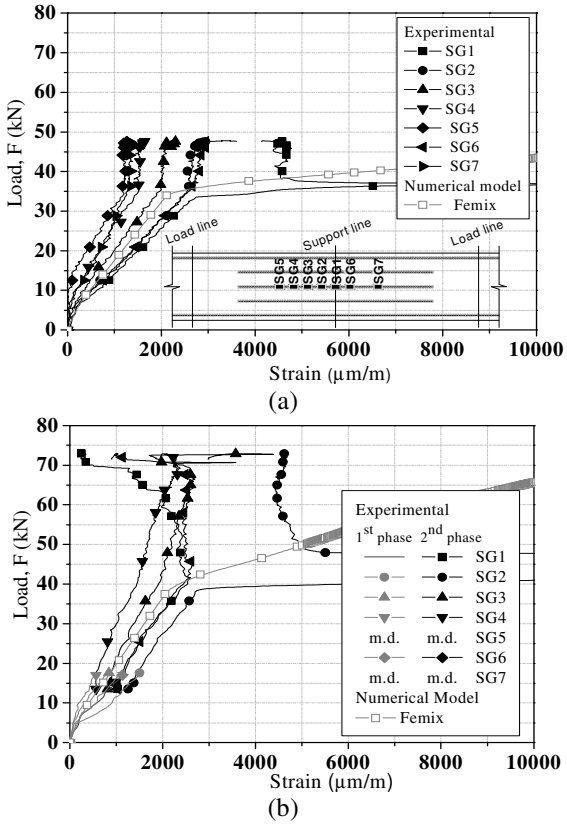

Figure 8: Force –strain relationships in steel at hogging region: (a) SL30 and (b) SL30s25.

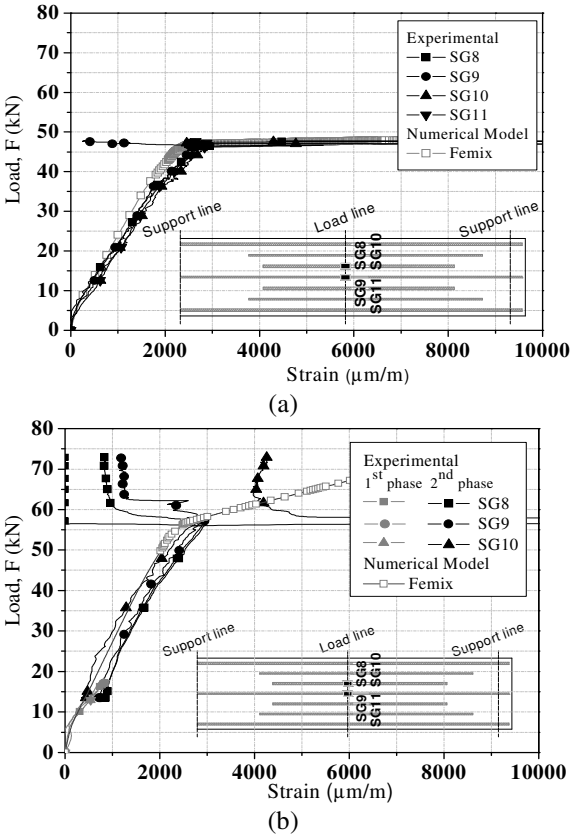

Figure 9: Force –strain relationships in steel at sagging region: (a) SL30 and (b) SL30s25.

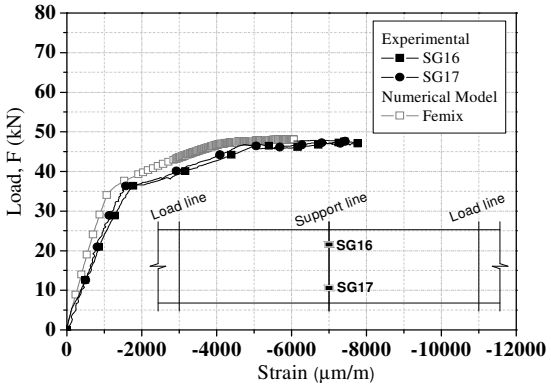

(a)

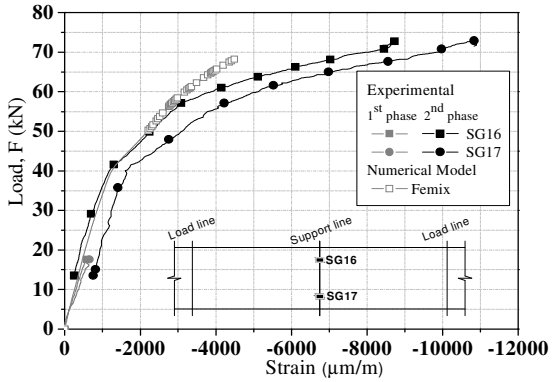

(b)

Figure 10: Force –strain relationships in concrete at hogging region: (a) SL30 and (b) SL30s25.

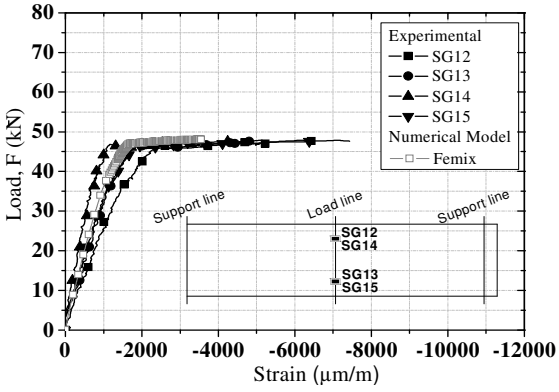

(a)

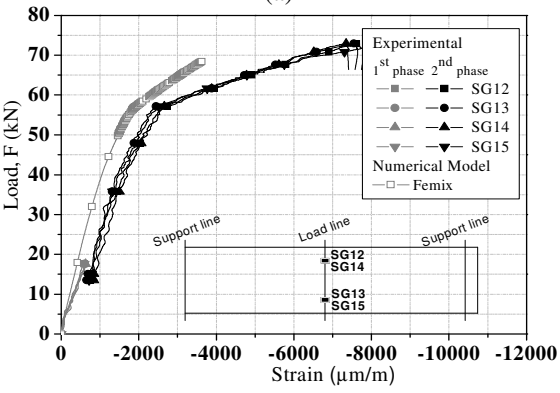

(b)

Figure 11: Force –strain relationships in concrete at sagging region: (a) SL30 and (b) SL30s25.

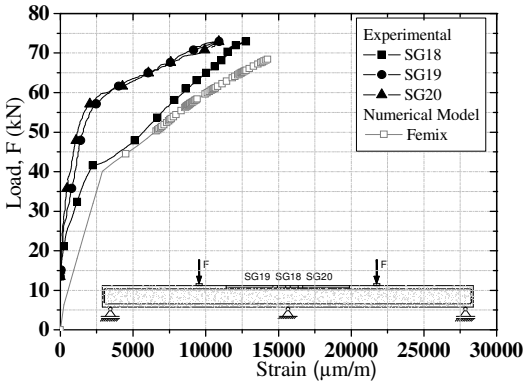

(a)

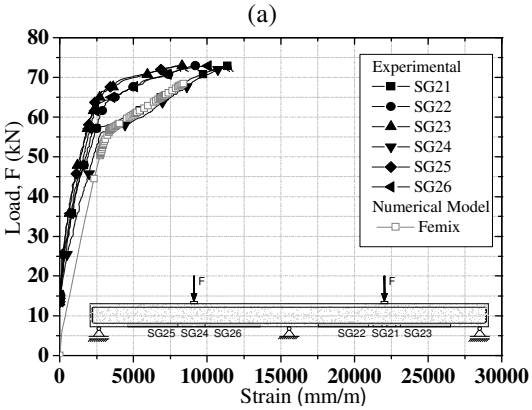

(b)

Figure 12: Force –strain relationships in CFRP laminates of SL30s25.

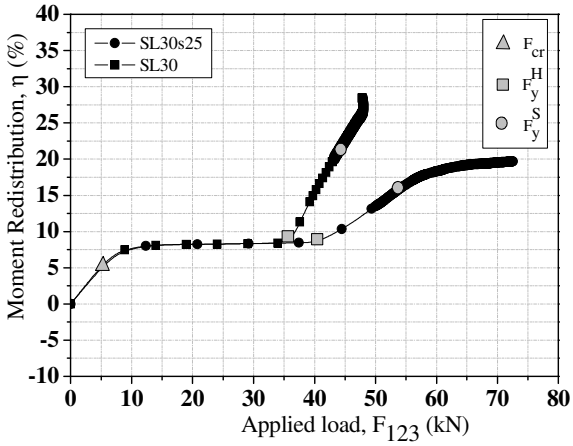

Figure 13: Moment redistribution-applied load relationship obtained numerically for the slabs.

Afterwards, a moment redistribution of 15.76% was obtained at the yielding of steel reinforcement at the sagging region. Finally, for a compressive strain of 3.5‰ at H and S, respectively, moment redistribution rates of about 18.22% and 19.37% were obtained.

Figure 14 shows the variation of the negative (M^-) and positive (M^+) moments with the increase of the applied load. The tendency of the M-F relationship to approximate to the elastic relationship when a 30% of moment redistribution was assumed indicates that the moment redistribution mechanism was formed.

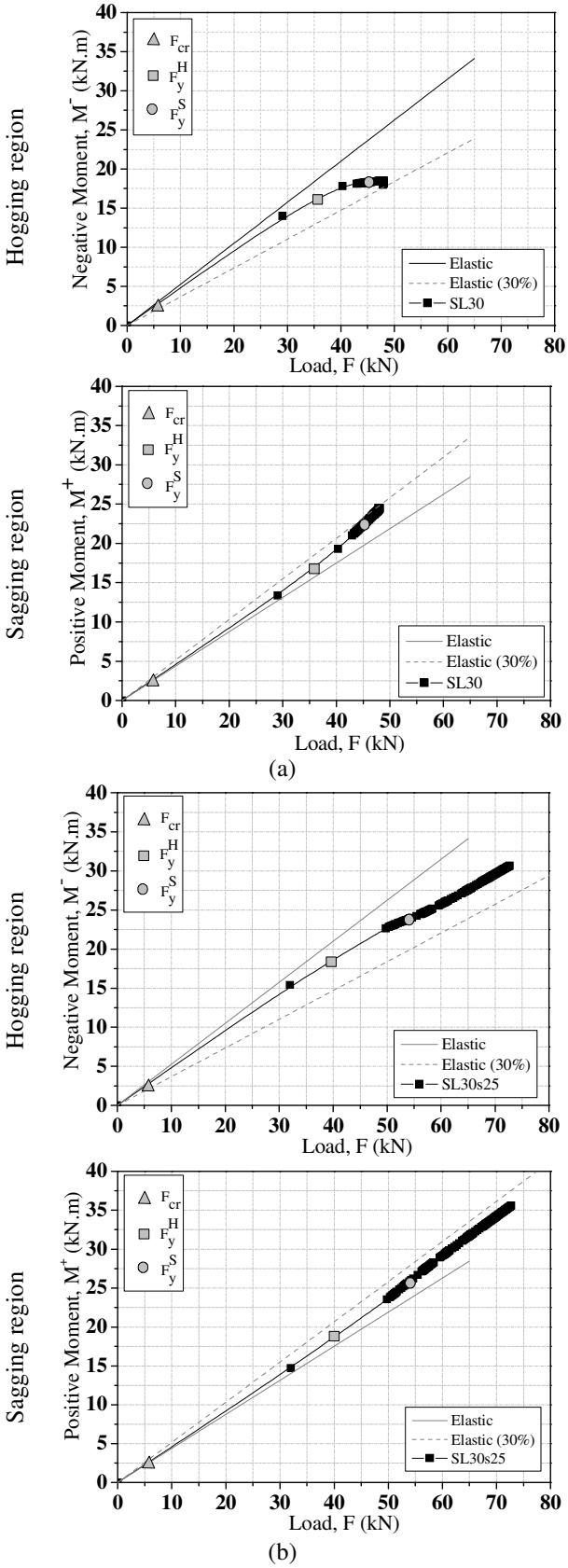

Figure 14: Bending moment -applied load relationship: (a) SL30 and (b) SL30s25.

CONCLUSIONS

This work deals with the use of the NSM CFRP laminates for the flexural strengthening of continuous RC slabs. The strengthening procedures adopted in the laboratory tests followed, as much as possible, the real strengthening practice for this type of interventions. The obtained results show that the proposed technique is able to increase the load carrying capacity of RC slabs and preserves relevant levels of moment redistribution. However, the load carrying capacity of the strengthened slab was limited by the detachment of the strengthened concrete cover layer at the intermediate support. For validation purposes, a computer program, based on the finite element method (FEM), was used. Using the obtained experimental results, the capability of the FEM-based computer program to predict with high accuracy the behaviour of this type of structures up to its collapse was highlighted.

FURTHER RESEARCH

Since many in situ RC structures are continuous constructions, this PhD program aims to conduct a more comprehensive investigation to examine the behaviour of continuous members with NSM CFRP laminates in both hogging/sagging regions. Once NSM strengthening can increase the flexural capacity up to a level higher than the shear capacity of the member, the load carrying capacity of the strengthened slabs can be limited by the detachment of the strengthened concrete cover layer at the intermediate support, or due to the formation of a shear failure crack in the hogging region. Therefore, the NSM flexural strengthening technique will be complemented with a hybrid strengthening strategy that avoids the occurrence of slab's shear failure and the premature detachment of the NSM laminates (Figure 15).

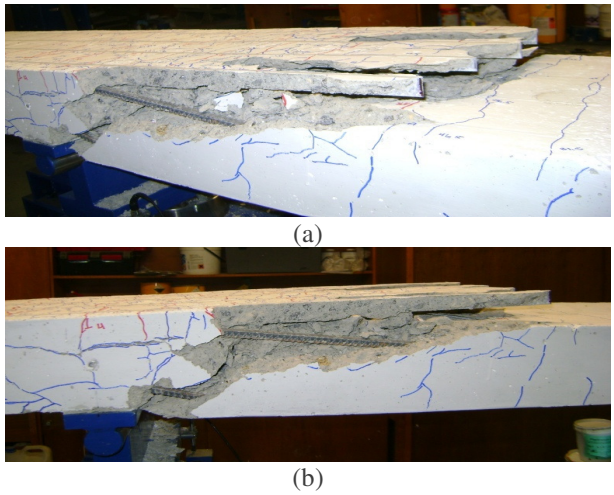

(a)

(b)

Figure 15: (a) Failure of the strengthened slab strip by the detachment of the strengthened concrete cover layer at the intermediate support/ the formation of a shear failure crack in the hogging region.

Brief description of the proposed experimental programs

To assess the effectiveness of the shear strengthening technique (ETS - Embedded Through-Section), sixteen statically determinate beams will be strengthened according to the ETS shear technique (Figure 16), where holes are opened through the beam thickness, with the desired inclinations, and bars are introduced into these holes and bonded to the concrete substrate with adhesive materials. The proposed method presents advantages over existing methods for shear strengthening, such as Externally Bonded Reinforcing (EBR) and Near Surface Mounted Technique (NSM), mainly in the case of slabs. Unlike EBR and NSM techniques (where the FRP is installed on the concrete cover of RC element), in the ETS technique the strengthening bars relies on the concrete core of the element, offering a greater confinement and improving the bonding performance.

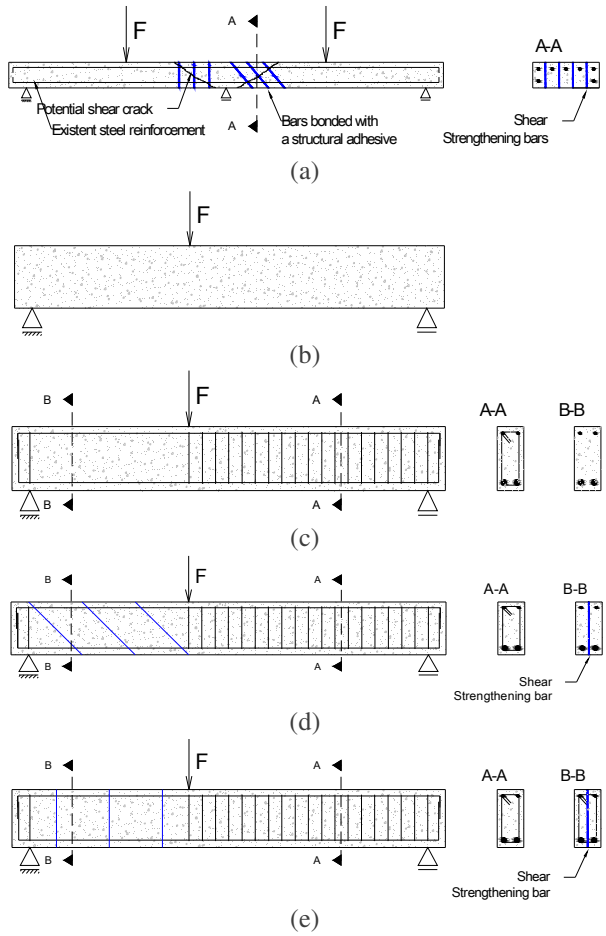

Figure 16: (a) Concept of the Embedded Through-Section (ETS) technique, (b) Typical specimen, (c) Reference beam and strengthening bars with the desired inclinations: (d) 45º and (e) 90º.

Afterwards, a comprehensive experimental program to evaluate the influence of relevant parameters for the effectiveness of a NSM/hybrid strengthening strategy on damaged concrete slabs will be carried out.

Continuous RC slab strips will be strengthened in flexure according to the NSM CFRP technique. Moreover, the influence of the hybrid strengthening technique (formed by combining the ETS technique with a method to prevent premature detachment of the NSM flexural strengthening bars) will be assessed. The strategy to avoid the premature detachment of the NSM laminates is an improvement in the ETS technique (Figure 17). A FRP strand will be used to stitch the strengthening bars and the CFRP laminate, increasing the confinement of the laminates. As previously mentioned, holes will be open through the slab thickness. Additionally, before the installation of the FRP laminates, notches will be cut in the top surface of the element, with a depth between 3 and 5 mm, in order that the strand stay above the laminates in the critical detachment region. The FRP strands and the strengthening bars will be positioned and, finally, bonded to concrete with an adhesive material.

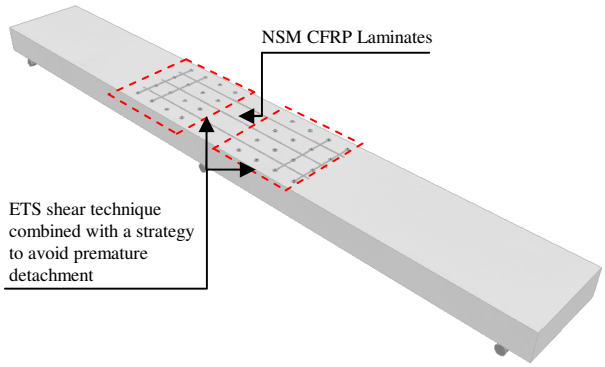

Figure 17: NSM/hybrid strengthening strategy:

Analytical Models

Finally, the PhD program aims the development of analytical models to design the (a) NSM flexural strengthening solutions for continuous RC beams/slabs, (b) ETS shear strengthening system for RC beams/slabs and (c) hybrid strengthening technique for continuous RC beams/slabs.

The ideia is to develop simple, but robust, analytical models able of providing high accurate numerical simulations that, giving the geometrical characteristics, the load configuration and the material properties of the intervening materials of a continuous RC beam/slab, can evaluate the NSM flexural strengthening solution (and predict if shear failure can occur) that assures a desired moment redistribution level and ductility performance.

ACKNOWLEDGEMENTS

The study reported in this paper forms a part of the research program "CUTINEMO - Carbon fiber laminates applied according to the near surface mounted technique to increase the flexural resistance to negative moments of continuous reinforced concrete structures" supported by FCT, PTDC/ECM/73099/2006. The first author would like to acknowledge the National Council for Scientific and Technological Development (CNPq) – Brazil for financial support for scholarship (GDE 200953/2007-9).

REFERENCES

ACI Committee 318. 2004. "Building code requirements for structural concrete and Commentary (ACI 318-04)", Reported by committee 318, *American Concrete Institute*, Detroit, 351 pp.

ACI Committee 440. 2007. "Guide for the design and construction of externally bonded FRP systems for strengthening concrete structures", *American Concrete Institute*, 118 p.

Anwarul Islam, A.K.M.. 2009. "Effective methods of using CFRP bars in shear strengthening of concrete girders", *Engineering Structures*, 31(3), pp. 709-714.

ASTM A370. 2002. "Standard test methods and definitions for mechanical testing of steel products", *American Society for Testing and Materials*.

Barros, J.A.O.. 1995. "Comportamento do betão reforçado com fibras - análise experimental e simulação numérica (Behavior of FRC – experimental analysis and numerical simulation)", PhD Thesis, Civil Eng. Dept., Faculty of Engineering, University of Porto, Portugal (in Portuguese).

Barros, J.A.O., Fortes, A.S.. 2005. "Flexural strengthening of concrete beams with CFRP laminates bonded into slits", *Journal Cement and Concrete Composites*, 27(4), pp. 471-480.

Barros, J.A.O., Dias, S.J.E.. 2006. "Near surface mounted CFRP laminates for shear strengthening of concrete beams", *Cement & Concrete Composites*, 28, pp. 276–292.

Barros, J.A.O., Dias, S.J.E., Lima, J.L.T. 2007. "Efficacy of CFRP-based techniques for the flexural and shear strengthening of concrete beams", *Journal Cement and Concrete Composites*, 29(3), 203-217.

Barros, J.A.O., Kotynia, R. (2008). "Possibilities and challenges of NSM for the flexural strengthening of RC structures", *Fourth International Conference on FRP Composites in Civil Engineering* (CICE2008), Zurich, Switzerland.

Barros, J.A.O.; Dalfré, G. M. ; Dias, A. A. 2008. "Numerical Simulation of Continuous RC Slabs Flexural Strengthened according NSM technique", *Proceedings of 2nd International Conference on Concrete Repair, Rehabilitation, and Retrofitting* (ICCRRR 2008), Alexander M.G. et al. (Eds.), Cape Town, South Africa, 24 – 26 November, pp. 387-388.

Bonaldo, E.. 2008. Composite materials and discrete steel fibres for the strengthening of thin concrete structures. PhD Thesis, University of Minho, Guimarães, Portugal.

CEB-FIP Model Code 1990. 1993. "Design Code". *Thomas Telford*, Lausanne, Switzerland.

De Lorenzis, L., A. Nanni, and A. La Tegola. 2000. "Strengthening of Reinforced Concrete Structures with Near Surface Mounted FRP Rods" , *bibl. International Meeting on Composite Materials*, PLAST 2000, Milan, Italy, May 9-11.

Dias, S.J.E., Barros, J.A.O. 2008. "Shear strengthening of T cross section reinforced concrete beams by near surface mounted technique", *Journal Composites for Construction*, 12(3), 300-311.

Dias, S.J.E.; Barros, J.A.O. 2010. "Performance of reinforced concrete T beams strengthened in shear with NSM CFRP laminates", *Engineering Structures*, 32(2), pp. 373-384.

FIB - Bulletin 14. 2001. "Externally bonded FRP reinforcement for RC structures", *Technical report by Task Group 9.3 FRP*, 130 p.

ISO 527-1. 1993. "Plastics - Determination of tensile properties - Part 1: General principles", *International Organization for Standardization* (ISO), Genèva, Switzerland, 9 p.

ISO 527-2. 1993. "Plastics - Determination of Tensile Properties - Part 2: Test Conditions for Moulding and Extrusion Plastics", *International Organization for Standardization* (ISO), Geneva, Switzerland.

ISO 527-5. 1993. "Plastics - Determination of tensile properties - Part 5: Test conditions for unidirectional fibre-reinforced plastic composites", *International Organization for Standardization* (ISO), Genèva, Switzerland, 9 p.

Liu, I.S.T. 2005. Intermediate crack debonding of plated reinforced concrete beams. PhD Thesis, School of Civil and Environmental Engineering, The University of Adelaide, Adelaide, Australia.

Liu, IST, Oehlers, DJ, and Seracino, R. 2006. Tests on the ductility of reinforced concrete beams retrofitted with FRP and steel near-surface mounted plates. Journal of Composites for Construction, 10(2): 106-114.surface mounted technique." In *Proceedings of the Fourth International Conference on FRP Composites in Civil Engineering* (Zurich, CH, Jul.22-24), 6 pp.

LNEC E397. 1993. Concrete—Assessment of the elasticity modulus under uniaxial compression. Laboratório Nacional de Engenharia Civil, (in Portuguese).

Sena-Cruz, J.M. 2004. "Strengthening of concrete structures with near-surface mounted CFRP laminate strips." PhD Thesis, Department of Civil Engineering, University of Minho.

GLÁUCIA DALFRÉ was born in Limeira, Brazil, and graduated in Civil Engineering by Piracicaba School of Engineering in 2004. Master of Science degree (MSc) in Civil Engineering by Sao Carlos School of Engineering (EESC), University of Sao Paulo (USP), Brazil, at February 2007.

She is a PhD Student of ISISE, Department of Civil Engineering, University of Minho, Portugal, since October 2007. Her research interests include structural analysis and modeling, fiber-reinforced composites, including repair and retrofit of civil infrastructures. Her e-mail address is gmdalfre@civil.uminho.pt.